The strong Stark effect of intersubband transitions in corrugated lateral surface superlattices

1998 J. Phys.: Condens. Matter 10 3783

(http://iopscience.iop.org/0953-8984/10/17/010)

J. Phys.: Condens. Matter **10** (1998) 3783–3790. Printed in the UK PII: S0953-8984(98)87574-7

The strong Stark effect of intersubband transitions in corrugated lateral surface superlattices

Hong Sun

CCAST (World Laboratory), PO Box 8730, Beijing 100080, People's Republic of China and Department of Physics and Institute of Condensed Matter Physics, Shanghai Jiao Tong University, Shanghai 200030, People's Republic of China†

Received 12 September 1997, in final form 14 January 1998

Abstract. Intersubband electro-absorption and electro-refraction index spectra of GaAs/AlAs corrugated lateral surface superlattices (CLSSLs) are calculated. Large shifts of intersubband transition energies and Fermi energy levels in the electron occupied subbands induced by applied electric fields result in strong intersubband Stark effects and large refractive index variations in the CLSSLs that we considered with moderate electric fields ($|F| \leqslant 100$ kV cm^{-1}). Strong intersubband absorptions with normally incident light due to the corrugated interfaces of the CLSSLs which break the in-plane translational symmetry of the systems are predicted. Broadenings of the intersubband electro-absorption and electro-refraction index spectra caused by structural fluctuations of the CLSSLs are discussed.

1. Introduction

Ever since the discovery of the large quantum-confined Stark effect (QCSE) in quantum wells [1], modulations of absorption coefficients and refractive indexes in low-dimensional electronic systems by external electric fields have attracted a great deal of attention because of the potential device applications in designing high-speed, low-driving-voltage optical modulators, switches and detectors. The QCSE in InAlGaAs/InGaAs and InAsP/GaInP multi-quantum wells (QWs) has been used to design high-speed, high-efficiency optical modulators operating near 1.06, 1.3 and 1.55 μm wavelengths [2–4] which have important applications in long-distance optical fibre communications. Voltage-tunable infrared photodetectors making use of the large Stark shifts of the strong intersubband absorptions in coupled QWs have been proposed [5]. And very recently, waveguide modulators based on the QCSE in II–VI semiconductor multi-QWs were fabricated [6–8]; the motivation for this development was their potential for monolithic integration with room-temperature II–VI semiconductor lasers operating in the blue/green spectral region. Investigations on the QCSE in different low-dimensional systems, such as quantum wires [9] and dots [10], are being carried out in searching for systems with strong Stark effects.

The rapid advances in modern microstructure technology have made it possible to fabricate two-dimensional (2D) electron systems with additional periodic modulations along their lateral directions. Structures with short lateral periods ($\sim$10 nm) comparable to the vertical dimension of these 2D systems have been produced by direct crystal growth methods, which include (i) deposition of GaAs and AlAs fractional layers on (001) GaAs

† Mailing address; e-mail: shong@mail.sjtu.edu.cn.

0953-8984/98/173783+08$19.50

vicinal surfaces [11]; (ii) direct molecular-beam-epitaxy growth of GaAs and AlAs layers on high-index GaAs surfaces [12]; and (iii) direct molecular-beam-epitaxy growth of GaAs quantum wells on cleaved facets of GaAs/AlAs superlattices [13]. These structures are often referred to as corrugated lateral surface superlattices (CLSSLs), since the lateral modulations arise from the corrugated interfaces separating the well and barrier materials of the systems. The corrugated interfaces of the CLSSLs not only break the in-plane translational symmetry of the 2D systems to allow strong intersubband optical absorptions with normally incident light, but also result in strong intersubband Stark effects as electric fields can change the strength of the lateral modulations easily by moving the electrons towards or away from the corrugated interfaces. In this paper, we present the results of a model calculation of the intersubband Stark effects in the GaAs/AlAs CLSSLs.

2. The model calculation

The CLSSL model is the same as the one that we considered in a previous paper [14] with only one of its interfaces being corrugated, which resembles the CLSSL fabricated by deposition of GaAs and AlAs fractional layers on (001) GaAs vicinal surfaces [11]. Considering the intermixing of GaAs and AlAs during the fabrication process, a simple cosine-shaped corrugated interface is assumed, instead of the square-well-shaped profile of the ideal case. The coordinate system is so chosen that the z-axis is perpendicular to the CLSSL with its upper interface corrugated along the x-direction. The geometry of the model is determined by the average width L_z of the CLSSL, the amplitude δL_z and the lateral period L_x of its corrugated interface.

The calculation is carried out with the theory that we developed previously [14]. In the effective-mass approximation, the eigenvalue equation and boundary conditions of an electron are obtained by requiring the first-order difference of the following functional to be equal to zero ($\delta L = 0$):

$$L[\psi] = \int \frac{\hbar^2}{2m_e(\boldsymbol{r})} \left\{ \left| \frac{\partial \psi(\boldsymbol{r})}{\partial \boldsymbol{x}} \right|^2 + \left| \frac{\partial \psi(\boldsymbol{r})}{\partial \boldsymbol{y}} \right|^2 + \left| \frac{\partial \psi(\boldsymbol{r})}{\partial \boldsymbol{z}} \right|^2 \right\} \mathrm{d}\boldsymbol{r} + \int [V(\boldsymbol{r}) + eFz] |\psi(\boldsymbol{r})|^2 \mathrm{d}\boldsymbol{r} - E \int |\psi(\boldsymbol{r})|^2 \, \mathrm{d}\boldsymbol{r} \tag{1}$$

where $m_e(\boldsymbol{r})$ is the electron effective mass, $V(\boldsymbol{r})$ is the band offset of GaAs and AlAs, F is the vertically applied electric field and E is the eigen-energy to be determined. To overcome the calculational difficulty due to the complicated boundary conditions of the electrons on the corrugated interface of the CLSSL, we introduce the same coordinate transformation as was used in reference [14], which transforms the CLSSL into a QW with planar interfaces plus an effective lateral periodic potential due to the corrugated interface. When a constant electric field is applied perpendicularly to the CLSSL, then, strictly speaking, no bound state exists if the barrier height of the CLSSL is finite. The electrons will finally tunnel out of the CLSSL. But the tunnelling becomes significant only in the CLSSLs with narrow well widths ($L_z < 5$ nm) or in high electric fields ($|F| > 200$ kV cm^{-1}) [15]. For the case of wide well widths ($L_z \approx 10$ nm) and intermediate electric fields ($|F| \approx 100$ kV cm^{-1}) in which we are interested, the tunnelling is negligible and (quasi-) bound states exist in the CLSSLs. The intersubband Stark effect in the CLSSLs is analysed by a perturbation method [15], where the effective potential due to the corrugated interface and applied electric field is considered as a perturbation of the Hamiltonian, while the bound states of the CLSSL are expanded in the eigen-wavefunctions of the corresponding QW in the

transformed space [14]. The method proves to be accurate in cases with no electric field [14] or no corrugated interface (QWs) [15]. In the calculation, the effects of the electron effective-mass discontinuity ($m_{\mathrm{GaAs}} = 0.0665m_0$ and $m_{\mathrm{AlAs}} = 0.124m_0$) and finite barrier height ($\Delta V_c = 1.06$ eV) between GaAs and AlAs are taken into consideration. The electron subbands of the CLSSLs in the electric field are obtained by diagonalizing the eigenvalue equation obtained from minimizing the functional $L[\psi]$ [14]. A sufficient number of the expansion functions are used in the numerical calculation to give a calculation accuracy of 1% for the first three subbands. Employing the Kramers–Kronig relation [16], the electron wavefunctions and subbands obtained are then used to calculate the absorption coefficients and refractive indexes associated with the intersubband transitions of the CLSSL in the electric field.

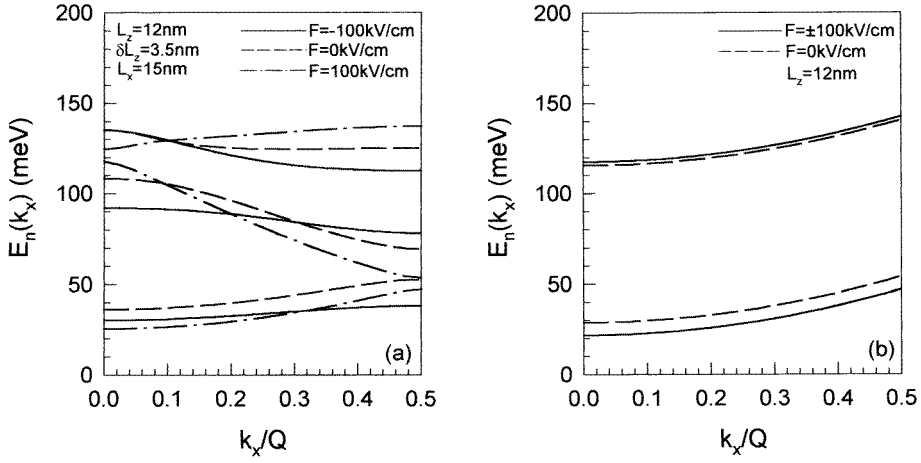

Figure 1. The first three electron subbands calculated for a GaAs/AlAs CLSSL with electric fields of $F = -100$, 0, 100 kV cm^{-1}, within the FBZ associated with the lateral period of the CLSSL ($Q = 2\pi/L_x$). The structural parameters of the CLSSL are $L_z = 12$ nm, $\delta L_z = 3.5$ nm and $L_x = 15$ nm. (b) The first two electron subbands calculated for a GaAs/AlAs QW with a well width of $L_z = 12$ nm in the same electric fields.

3. Results

In figure 1(a), we give the first three electron subbands calculated for a GaAs/AlAs CLSSL with electric fields of $F = -100$, 0, 100 kV cm^{-1} within the first Brillouin zone (FBZ) associated with the lateral period of the CLSSL ($Q = 2\pi/L_x$). The structural parameters of the CLSSL are $L_z = 12$ nm, $\delta L_z = 3.5$ nm and $L_x = 15$ nm. Also given, in figure 1(b), are the first two electron subbands calculated for a GaAs/AlAs QW with a well width of $L_z = 12$ nm in the same electric fields. The subbands in the CLSSL depend much more sensitively on the electric fields than those in the QW. This is because the first few subbands of the CLSSL that we considered result from the electron coherent scatterings by the periodically corrugated interface in the lateral x-direction. The electric fields can increase or decrease the coherent scatterings (or the lateral modulation) effectively by moving the electrons in the CLSSL towards ($F = -100$ kV cm^{-1}) or away from ($F = 100$ kV cm^{-1}) the corrugated interface. One should also note that the electric fields not only change the subband gaps, but also modify (flatten or curve) the dispersion relations of the subbands of

the CLSSL (figure 1(a)), while in the QW the electric fields cause only parallel shifts of the subbands (figure 1(b)). This difference is important in explaining the strong Stark effect of the intersubband absorptions in the CLSSLs.

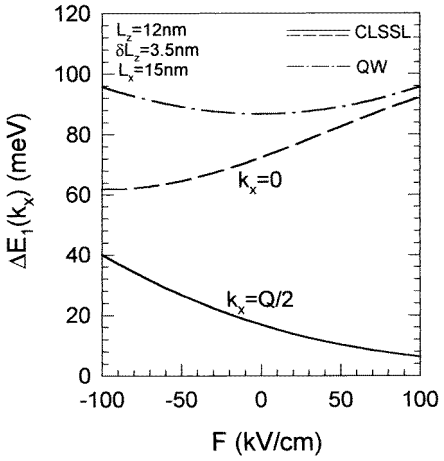

Figure 2. The intersubband transition energy $\Delta E_1(k_x) = E_2(k_x) - E_1(k_x)$ as functions of the electric field F at $k_x = 0$ and $k_x = Q/2$ calculated for the same CLSSL and QW as for figure 1.

The sensitive dependence of the subbands of the CLSSL on the applied electric fields is shown more clearly in figure 2 where we give the calculated intersubband transition energy $\Delta E_1(k_x) = E_2(k_x) - E_1(k_x)$ as functions of the electric field F at $k_x = 0$ and $k_x = Q/2$ for the same CLSSL and QW as for figure 1. The Stark shifts of the intersubband transition energies in the CLSSL are much larger than those in the QW.

In figure 3, we give the calculated optical absorption coefficients $\alpha(\hbar\omega)$ (figures 3(a), 3(c)) and refractive indexes [16] $n(\hbar\omega)$ (figures 3(b), 3(d)) associated with the intersubband transitions in the same CLSSL, as functions of the energy $\hbar\omega$ of the incident light which is polarized in the directions parallel (figures 3(a), 3(b) where $e_x = 1$) or perpendicular (figures 3(c), 3(d) where $e_z = 1$) to the CLSSL. The electron density in the CLSSL is $N = 5 \times 10^{11}$ cm^{-2}. Stark shifts as large as 35 meV and strong refractive index variations are expected in the CLSSL as the electric field varies from -100 to 100 kV cm^{-1}.

To analyse the absorption processes in the CLSSL, we plot in figure 4 the square of the calculated momentum matrices $|\boldsymbol{e} \cdot \boldsymbol{P}_n(k_x)|^2$ for the intersubband transitions from the lowest to the higher subbands ($n = 2, 3, \ldots$), where $\boldsymbol{e}$ is the polarization unit vector of the incident light. It is clear from figure 4 that for the incident light polarized parallel to the CLSSL (figure 4(a) where $e_x = 1$), such as for normal incidence, the absorption peaks in figure 3(a) are mainly due to the electron transitions from the lowest ($n = 1$) to the first excited subband ($n = 2$) at the edge of the FBZ ($|k_x| \approx Q/2$), while for the incident light polarized perpendicular to the CLSSL (figure 4(b) where $e_z = 1$), the absorption peaks in figure 3(c) correspond to the transitions from the lowest to the first excited subband at the centre of the FBZ ($|k_x| \approx 0$) and second excited subband ($n = 3$). The strong intersubband absorptions with the normally incident light (figure 3(a)) show the difference of the selection rules for the CLSSLs from those for the conventional QWs, where the intersubband absorptions vanish for the incident light polarized parallel to the QWs due to their in-plane translational symmetry. The corrugated interfaces in the CLSSLs break the translational symmetry and make the forbidden transitions become allowed ones.

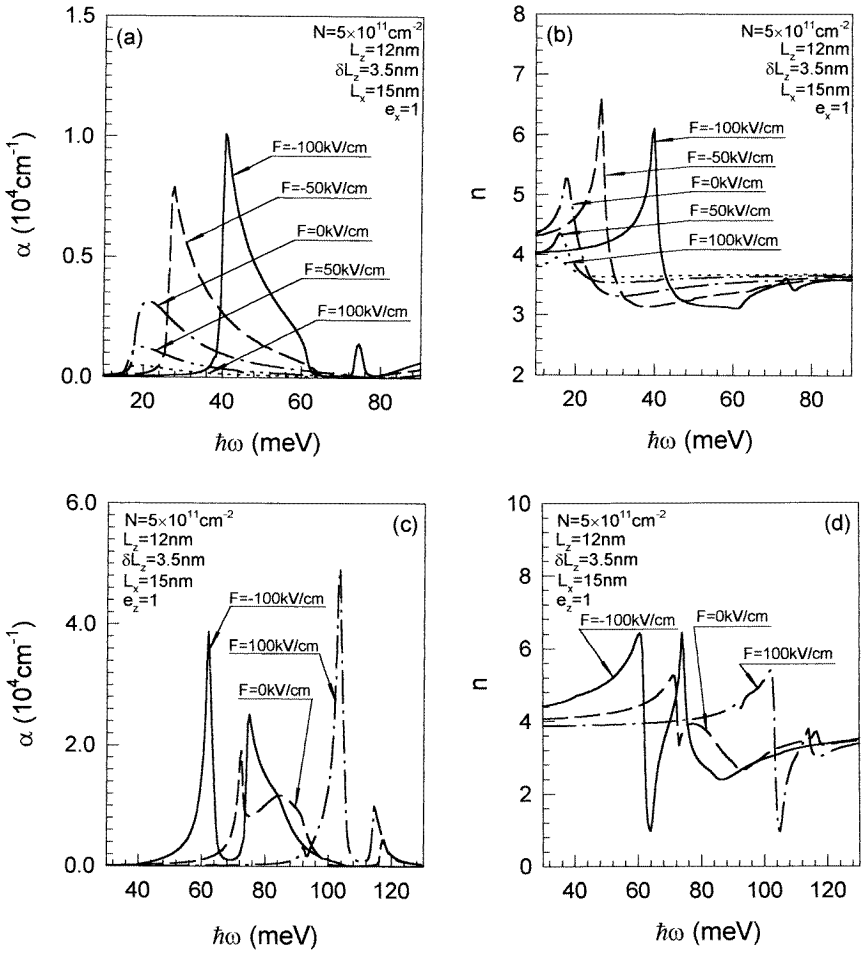

Figure 3. The optical absorption coefficients α ((a), (c)) and refractive indexes n ((b), (d)) associated with the intersubband transitions, calculated for the same CLSSL as for figure 1, as functions of the energy of the incident light which is polarized in the directions parallel ((a), (b)) or perpendicular ((c), (d)) to the CLSSL. The electron density in the CLSSL is $N = 5 \times 10^{11}$ cm^{-2}.

Besides the large Stark shifts of the absorption peaks, the electric fields also affect the intersubband absorptions in the CLSSL by changing the Fermi energy level relative to the subband structure. For the CLSSL shown in figure 3(a) with an electron density $N = 5 \times 10^{11}$ cm^{-2}, the Fermi energy level moves from outside to inside the lowest subband as the electric field varies from -100 to 100 kV cm^{-1}, due to the modification of the subband dispersion relations of the CLSSL by the electric fields (see figure 1(a)). The strong absorption peaks and large refractive index variations associated with the electron intersubband transitions near the edge of the FBZ ($|k_x| \approx Q/2$) disappear as the Fermi level moves into the lowest subband of the CLSSL, emptying the electron states near the edge of the FBZ (see figures 3(a), 3(b)). The electric fields not only shift the peak positions, but also change greatly the strength of the intersubband absorptions in the CLSSLs. This Fermi energy modification of the intersubband absorptions by the electric

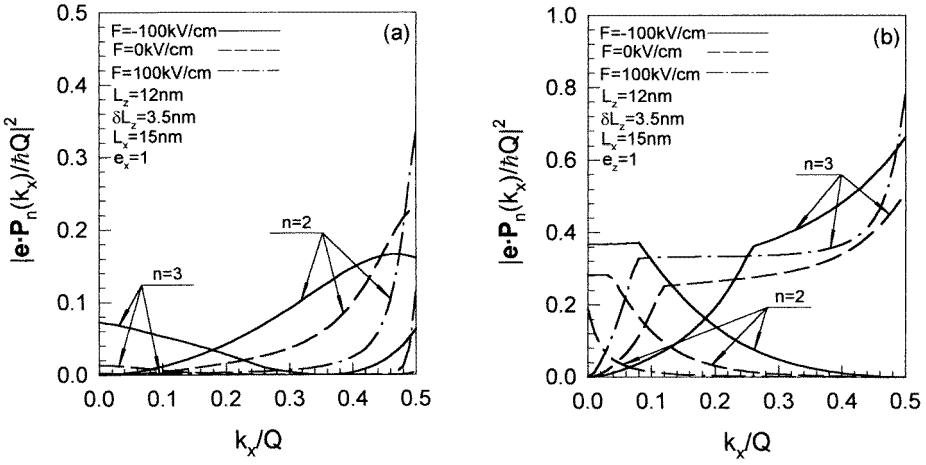

Figure 4. The square of the momentum matrices $|\boldsymbol{e}\cdot\boldsymbol{P}_n(k_x)|^2$ for the intersubband transitions from the lowest to the higher subbands ($n = 2, 3, \ldots$), calculated for the same CLSSL as for figure 1 with the polarization unit vector $\boldsymbol{e}$ of the incident light parallel (a) or perpendicular (b) to the CLSSL.

fields does not occur for the QW with planar interfaces. The subband energy of the QW is $E_n(k_x, k_y) = \epsilon_n(F) + \hbar^2k^2/2m_e$, where $\epsilon_n(F)$ is the energy level for the electron motion in the direction perpendicular to the QW. $\epsilon_n(F)$ depends on the vertically applied electric field F. For a given density N of the electrons, it is easy to show that the Fermi energy of the QW is $E_F = \epsilon_1(F) + \pi\hbar^2N/m_e$, if the electrons occupy only the lowest electron subband. The relative position $E_F - \epsilon_1(F)$ of the Fermi energy in the electron occupied subband does not change as the applied electric field F changes.

Fluctuations in the CLSSL geometry structures, which are inevitable during the

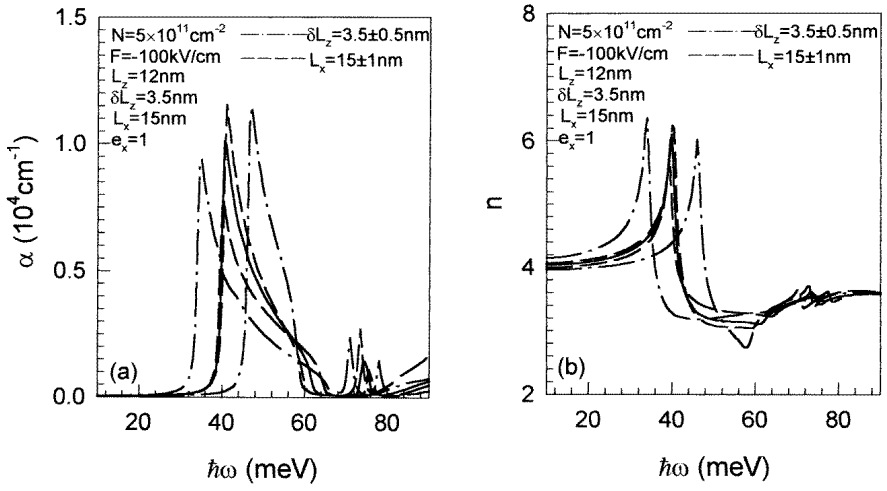

Figure 5. The intersubband absorption (α) and refractive index (n) spectra calculated for the same CLSSL as for figure 3 except with $L_x = 15 \pm 1$ nm or $\delta L_z = 3.5 \pm 0.5$ nm. The electric field is $F = -100$ kV cm^{-1}. The polarization of the incident light is $e_x = 1$.

fabrication processes, will broaden or even smear out the intersubband absorption spectra of the CLSSLs. The intersubband absorptions usually exhibit more sensitive dependence on the CLSSL structures than the interband absorptions, as the latter are mainly determined by the conduction–valence-band gap of the bulk materials, while the former are due entirely to the specific structures of the CLSSLs. The experimental observation of the former requires higher quality for the CLSSL samples. Estimations of the broadenings in the intersubband absorption and refractive index spectra due to the structural fluctuations of the CLSSLs are shown in figure 5, where we plot the calculated intersubband absorption coefficient α and refractive index n (with $F = -100$ kV cm^{-1} and $e_x = 1$) for the same CLSSL as for figure 3 except with $L_x = 15 \pm 1$ nm or $\delta L_z = 3.5 \pm 0.5$ nm. It is estimated that to observe the predicted intersubband Stark effect, the structural fluctuations of the CLSSLs must not be larger than 10%, which presents a challenge to the experimentalists as regards the fabrication of the CLSSL samples.

4. Conclusions

The intersubband electro-absorption and electro-refraction index spectra of the GaAs/AlAs CLSSLs are calculated. The large shifts of the intersubband transition energies and Fermi energy level in the electron occupied subband induced by the applied electric fields result in strong intersubband Stark effects and large refractive index variations in the CLSSLs that we considered with moderate electric fields ($|F| \leqslant 100$ kV cm^{-1}), which shows the CLSSL structure to be very promising as regards designing optoelectronic devices for operation in the infrared region. Strong intersubband absorptions with normally incident light are expected due to the corrugated interfaces of the CLSSLs which break the in-plane translational symmetry of the systems. Because of the sensitive dependence of the electron subbands on the structures of the CLSSLs, high-quality CLSSL samples with small structural fluctuations must be fabricated in order to observe the predicted Stark effects in the CLSSLs.

Acknowledgments

This work was supported by the National Natural Science Foundation of China and a Direct Grant for Research from the Chinese University of Hong Kong under contract 2060137. The author is grateful to Professor K W Yu for instructive discussions on the subject and hospitality received during his stay in the Chinese University of Hong Kong.

References

[1] Miller D A B, Chemla D S, Damen T C, Gossard A C, Wiegmann W, Wood T H and Burrus C A 1984 *Phys. Rev. Lett.* **53** 2173
[2] Fan C, Shih D W, Hansen M W, Esener S C and Wieder H H 1993 *IEEE Photon. Technol. Lett.* **5** 1383
[3] Mei X B, Loi K K, Wieder H H, Chang W S C and Tu C W 1996 *Appl. Phys. Lett.* **68** 90
[4] Zhang L M and Carroll J E 1994 *IEEE J. Quantum Electron.* **30** 2573
[5] Huang Y M and Lien C H 1995 *J. Appl. Phys.* **78** 2700
[6] Thompson P J, Wang S Y, Horsburgh G, Steele T A, Prior K A and Cavenett B C 1996 *Appl. Phys. Lett.* **68** 946
[7] Toropov A A, Shubina T V, Ivanov S V, Lebedev A V, Sorokin S V, Oh E S, Park H S and Kopev P S 1996 *J. Cryst. Growth* **159** 463
[8] Short S W, Xin S H, Lou A, Yin H, Dobrowolska M and Furdyna J K 1996 *J. Electron. Mater.* **25** 253

[9] Sa'ar A, Givant A, Calderon S, Benshalom O, Kapon E, Gustafsson A, Oberli D and Caneau C 1996 *Superlatt. Microstruct.* **19** 217
[10] Jaziri S, Bastard G and Bennaceur R 1993 *J. Physique* IV **3** 367
[11] Tsuchiya M, Gaines J M, Yan R H, Simes R J, Holtz P O, Coldren L A and Petroff P M 1989 *Phys. Rev. Lett.* **62** 466
[12] Nötzel R, Ledentsov N N, Däweritz L, Hohensten M and Ploog K 1991 *Phys. Rev. Lett.* **67** 3812
[13] Akiyama H, Someya T and Sakaki H 1996 *Phys. Rev.* B **53** R4229
[14] Sun H, Huang J M and Yu K W 1996 *J. Phys.: Condens. Matter* **8** 7605
[15] Lengyel G, Jelley K W and Engelmann R W H 1990 *IEEE J. Quantum Electron.* **26** 296
[16] Johnson N F, Ehrenreich H, Hui P M and Yong P M 1990 *Phys. Rev.* B **41** 3655